SILICON AVALANCHE PHOTODIODES ARRAY FOR PARTICLE DETECTOR: MODELLING AND FABRICATION

Alexandre Khodin[†], Dmitry Shvarkov[‡], Valery Zalesski[†]

[†] Institute of Electronics, National Academy of Sciences of Belarus

Fax: +375-17-2652541, e-mail: hodin@mailcity.com

[‡] Institute of Nuclear Problems, Belarus State University

ISTC B-231-99 Project

Minsk - June, 2000

Large-area arrays (30x30) of metal/resistive layer/silicon (MRS) avalanche photodiodes as 150x150 micrometers sub-pixels are developed and fabricated to detect short-wavelength scintillator's signals for high-energy particles detection. Modelling of MRS photodiodes was performed using McIntyre' approach of local electric field to optimize semiconductor doping profiles and resistive layer parameters to obtain the minimum value of effective k-factor less than 0.01 under low excess noise factor and high gain. The resistive layer/silicon surface barrier suppresses minority carriers injection to decrease dark current and effective k-factor. Test samples of silicon avalanche photodiodes arrays have been fabricated using low-rate epitaxial growth of silicon layer, doping, and resistive layer deposition processing. The integral gain for experimental specimens was ~100.

Special thanks to:

Dr. Jean-Pierre Peigneux, LAPP/IN2P3, Annecy-Le-Vieux, France

The aim of the study in the frames of the ISTC Project B-231 is to develop and fabricate large-area detectors of short-wavelength photons (~0.4 μm) originated by a scintillator [1]. This paper presents intermediate results on modelling and fabrication of experimental specimens.

Two main versions of avalanche photodiodes based on resistive layer/silicon (RS) structure were investigated. The first type presents surface-barrier structure of resistive layer on silicon. Dark current density i_d is caused by two main components in this case: surface-barrier saturation current i_s and space charge region generation current i_g:

$$i_s = A^* \cdot T^2 \cdot \exp\left[-\frac{\phi_b}{kT} \right] \tag{1}$$

where: A^* - modified Richardson constant, ϕ_b - RS surface barrier height. The ϕ_b value varies to some extent for different materials of the resistive contact layer and is not known for some of them; as a reasonable approximation we took ϕ_b=0.7 eV which is characteristic of Ni/Si or $NiSi_x$/Si contact [2] ($NiSi_x$ formation temperature is between 473K and 673K, thus, it could be formed even under low-temperature subsequent processing). The i_g component, supposing generation rate constant in space charge region, is [2]:

$$i_g \approx \frac{q \cdot n_i \cdot W(U)}{\tau_{ef}} \tag{2}$$

where $W(U)$ is space charge region width depending on applied voltage U, τ_{ef} is effective carriers lifetime for this generation process, which is determined by deep impurities concentration N_t and kinetics parameters in the region. Supposing one kind of traps only, which are positioned far enough from the middle of the gap E_i in its upper part, we obtain:

$$\tau_{ef} = \frac{1}{v_{th} \cdot N_t \cdot \sigma} \exp\left(\frac{E_t - E_i}{kT} \right) \tag{3}$$

where $v_{th} = \left(3kT / m^*\right)^{1/2}$ is carriers thermal velocity, and σ - effective capture cross-section. N_t is supposed constant in the active region. The advantage of surface barrier structure is in low saturation current due to relatively high potential barrier at the RS interface. This would lead to a lower dark current as compared with p-n junction. And surface-barrier structure is more suitable for near-ultraviolet photons detection.

The second version of the structure studied contains shallow asymmetric p^+-n junction beneath the resistive layer. In this case:

$$i_s = q \cdot \sqrt{\frac{D_n}{\tau_n}} \cdot \frac{n_i^2}{N_A}, \tag{4}$$

where standard designations for electrons diffusion coefficient and lifetime are introduced, as well as doping impurity concentration in highly-doped region of the junction. As initial estimation, $\sigma \sim 10^{-14}$ см^2 value may be used [3], and traps concentration $N_t \sim 10^{11}$ cm^{-3}. Then, effective lifetime will be $\sim 10^{-4}$ s, and generation current density $i_g \sim 10^{-9}$ A·cm^{-2}. Using Einstein relation, we get for our case ($N_A = 10^{16}$ cm^{-3}, $\tau_n = 1 \cdot 10^{-6}$ s) the saturation current density $i_s = 3 \cdot 10^{-12}$ A·cm^{-2}. Thus, overall dark

current density consists of two main components, the former being dependent on applied voltage. For this reason, it seems reasonable to maintain overall space charge region width as narrow as possible for given spectral range of radiation detected, but do not shorten the part of this region with maximum electric field, where avalanche multiplication occurs.

2.

Computer modelling of MRS photodiode structures was performed using McIntyre' approach of local electric field [4] to optimize semiconductor doping profiles and resistive layer parameters to obtain the minimum value of effective K-factor (holes to electrons ionization coefficients ratio in the conditions of self-stabilized avalanche regime) to less than 0.01 under low excess noise factor F and high gain M.

The following physical and processing parameters of the structures under study were varied to establish optimum processing regimes:

- uniform doping level and thickness of base (epitaxial) layer,
- p-region doping profile to form a p-n junction,
- resistive layer specific layer resistivity,

Based on the model developed, the following output parameters of avalanche MRS structures were calculated:

- multiplication factor M,
- integral effective ratio K of holes to electron ionization coefficients β and α, correspondingly,
- noise factor F,
- current density I.

Calculation procedure for one-dimensional task included:

1. Silicon doping profile calculation using predetermined processing parameters: base doping level, epitaxial layer thickness, p- and n-regions doping processing parameters.
2. Preliminary estimation of one-dimensional profiles of electrostatic potential and field.
3. Doping parameters variation to obtain electric field profile with maximum value not exceeding $\approx 2.5 \cdot 10^5$ V/cm for a maximum depth interval.
4. Preliminary calculation of M, α, β, and K depth profiles to narrow the search region.
5. Iteration procedure implementation using predetermined values of external applied voltage V and resistive layer resistance R to calculate M, K, I, and F.
6. As a result of calculations were the M(V, R), K(V, R), and F(V, R) maps and dependencies for various doping profiles in silicon, enabling to optimize resistive layer and silicon doping parameters to gain maximum M and K values under minimum noise-factor F.

Calculation scheme and procedure included the following basic approaches and formulas. Taking into account that we try to restrict the maximum electric field value in the avalanche multiplication region, we use the history-independent McIntyre' approach of local electric field contrary to short structures [5]. The electric field and depth dependencies of electrons and holes ionization coefficients $\alpha(x,E)$ and $\beta(x,E)$ were calculated using the following expressions [6]:

$$\alpha(x,E) = 2.3 \cdot 10^5 \cdot \exp\left[-6.78 \cdot \left(\frac{2 \cdot 10^7}{E(x)} - 1 \right) \right] \tag{5}$$

$$\beta(x,E) = 1.3 \cdot 10^3 \cdot \exp\left[-13.2 \cdot \left(\frac{2 \cdot 10^7}{E(x)} - 1 \right) \right] \tag{6}$$

where E=E(x) is electric field profile in the depletion region. Dimensions are: E – V/m, α and β – m^{-1}.

Then, using α(x,E) and β(x,E) profiles, the calculation of multiplication factor M(E) effective K-factor the noise-factor F was performed:

$$M(E) = \left[1 - \int_W \alpha(x,E) \cdot \exp\left(- \int_W (\alpha(y,E) - \beta(y,E)) dy \right) dx \right]^{-1} \quad (7)$$

$$K(E) = \frac{\int_W \beta(x,E) \cdot M^2 dx}{\int_W \alpha(x,E) \cdot M^2 dx} \quad (8)$$

$$F(E) = K \cdot M + (2 - 1/M) \cdot (1 - K) \quad (9)$$

After preliminary estimation of M, K, and F in accordance with a selected initial doping profile, the iteration procedure was performed using predetermined values of resistive layer areal resistivity R and applied voltage V to calculate the active layer voltage drop U and corresponding applied electric field E. The iteration procedure to determine the operating regime of MRS-structure was based on self-consistent solution of transcendental equation for active region voltage drop U:

$$U = V - R \cdot (i_{ph} + i_d(U)) M(U) \quad (10)$$

where M(U) is field-dependent carriers multiplication factor in accordance with (7), i_{ph} is initial photocurrent density.

As a result, the M(V, R), K(V, R), and F(V, R) dependencies have been obtained as a basis for selection of resistive layer parameters and modified doping profile to achieve optimum relation between multiplication coefficient and noise factor of the devices.

The examples of calculated dependencies of MRS APD output parameters on resistive layer resistance and applied voltage are shown in Figs.1-3.

3.

The final step was optimization of'planar inhomogeneity of large-area MRS avalanche structures. An example of potential distribution map in single MRS APD sub-pixel (150 x150 micrometers) of the array under local photo-excitation is shown in fig.4. The pixel has only a local resistive contact to decrease light signal losses.

Test samples of silicon avalanche photodiodes arrays have been fabricated using silicon layer low-rate epitaxial growth, impurity implantation, and resistive layer deposition processing. Resistive layer materials were Ni, SiC, and ITO. The array contained 30x30 sub-pixels, each sub-pixel being 150x150 micrometers in size (fig.5). The output characteristics of the array are shown in fig.6.

4. Appendix

The ultimate pixel size in particle and photon detectors, could be reduced to nanometer level. We investigate discrete electrons transport in nano-arrays of quantum dots (fig.7) [7]. Such structures are considered as single-electron devices controlled by the effect of Coulomb blockade. Particle or

high-energy photon impact on a single dot could change its state due to direct ionization, Compton effect, or indirect quantum interference effects. Then, this dot will control electron transport between source and drain. Such devices promise high sensitivity to charged and uncharged particles and photons.

References

1. V.Zalessky, T.Leonova, V.Pan, M.Korzhik, O.Misevich, D.Shvarkov. In: "Scientific Research Conversion in Belarus in the frames of ISTC Activity". Intern.Seminar Materials. Minsk, May 17-22,1999. Part 1. pp.182-185.
2. S.M. Sze, Physics of semiconductor devices. Wiley&Sons, 1981.
3. E. Schibli, A.G. Milnes. Mater.Sci. Eng., **2**, 229 (1968).
4. R.J.McIntyre. IEEE Trans.Electron Devices, vol.ED-19, pp.703-713, 1972.
5. R.J.McIntyre. A new look at impact ionization – Part I. IEEE Trans. on El. Dev. Vol.46, No.8, 1999.
6. Y. Musienko. Simple model for EG&G APD. CMS NOTE 1998.
7. A.Khodin. On modeling of electronic and photoelectronic processes in nanostructures. Physics, Chem. and Appl. of Nanostructures. Ed. V.E.Borisenko, A.B.Filonov, S.V. Gaponenko, V.S.Gurin. World Scientific, Singapure etc. 1997, p.113-116.

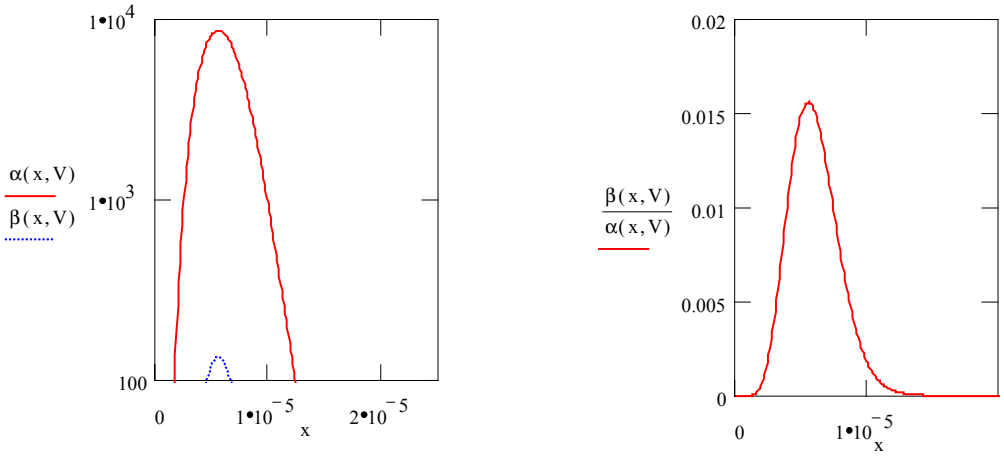

Fig.1. Depth profiles of electrons and holes ionization coefficients α and β (in cm^{-1}) and their ratio (x – in meters) for MRS APD structure with active layer thickness 20 micrometers and junction depth 5.5 micrometers.

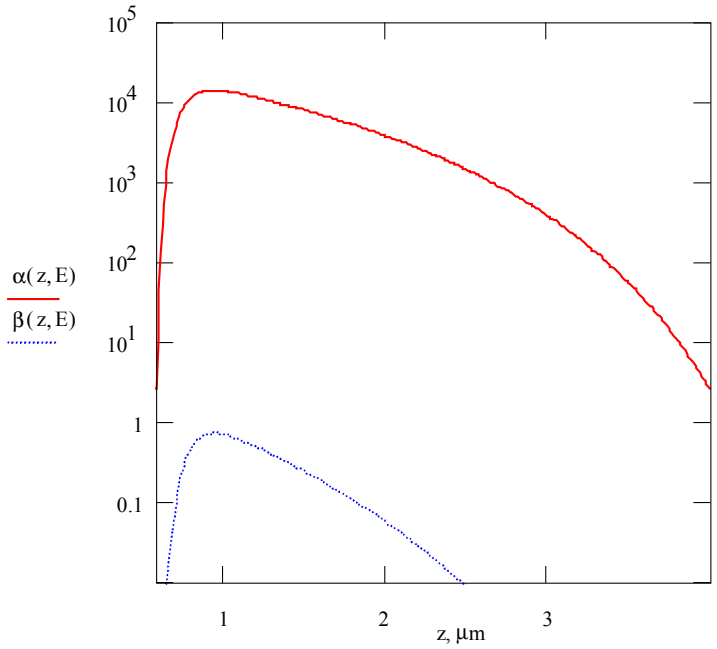

Fig.2. Electrons and holes ionization coefficients α and β (in cm^{-1}) depth profiles for MRS APD structure with active layer thickness 4 micrometers and junction depth 0.9 micrometers.

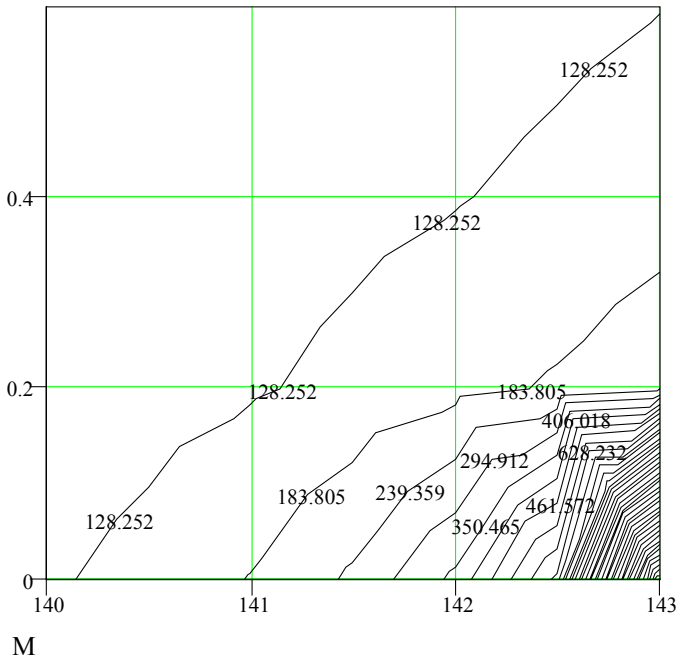

Fig.3. Multiplication coefficient M map versus applied voltage V (abscissa, Volts) and resistive layer areal resistance R (ordinate, Ohm·m^2)

Table

Epi-layer thickness, micrometers	p-n junction depth, micrometers	Output parameters	
		K	M
10	1.6	0.0034	200
	5.5	0.0023	280
4	0.8	0.0026	210
	1.4	0.0017	230

Fig.4.

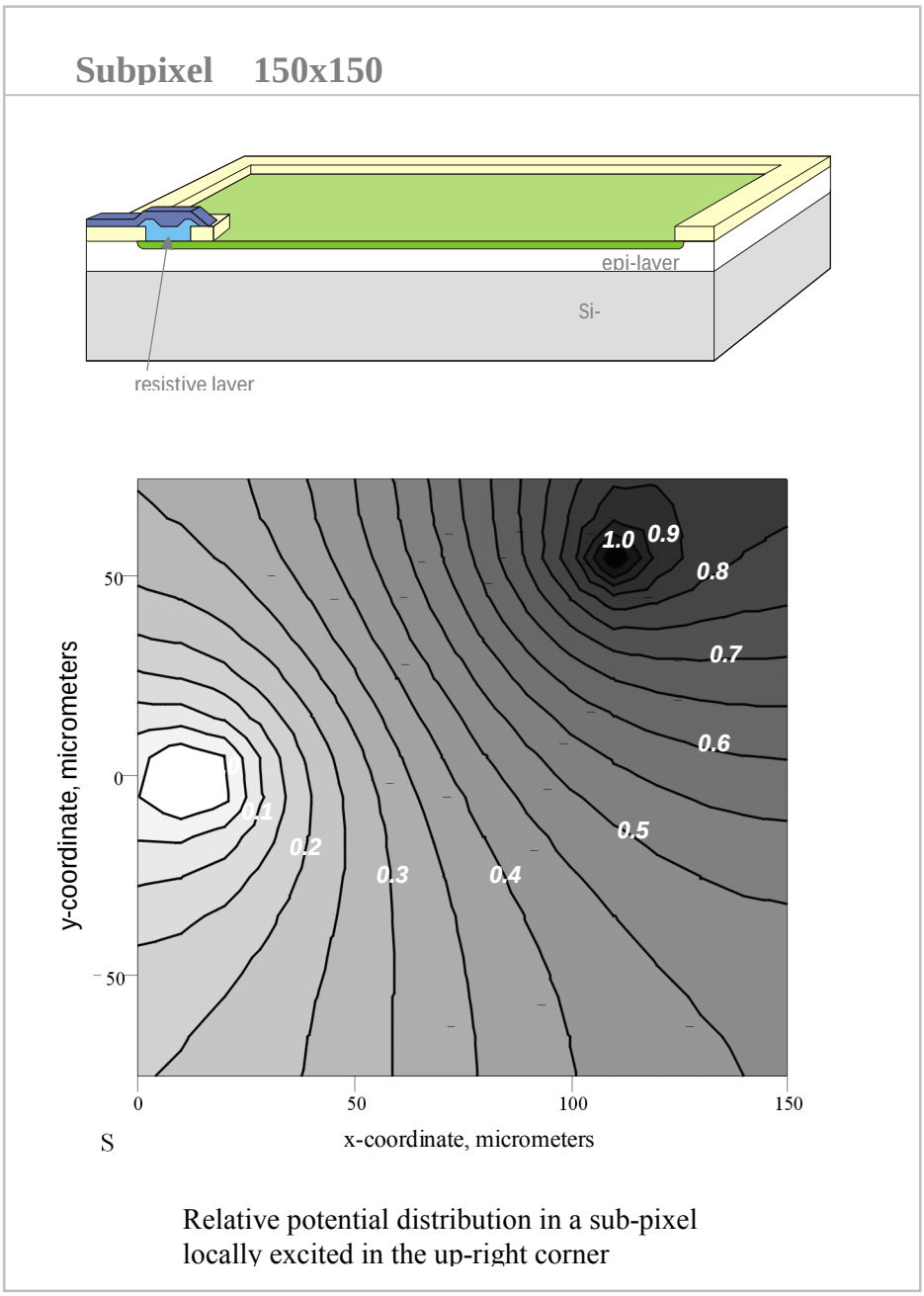

Relative potential distribution in a sub-pixel locally excited in the up-right corner

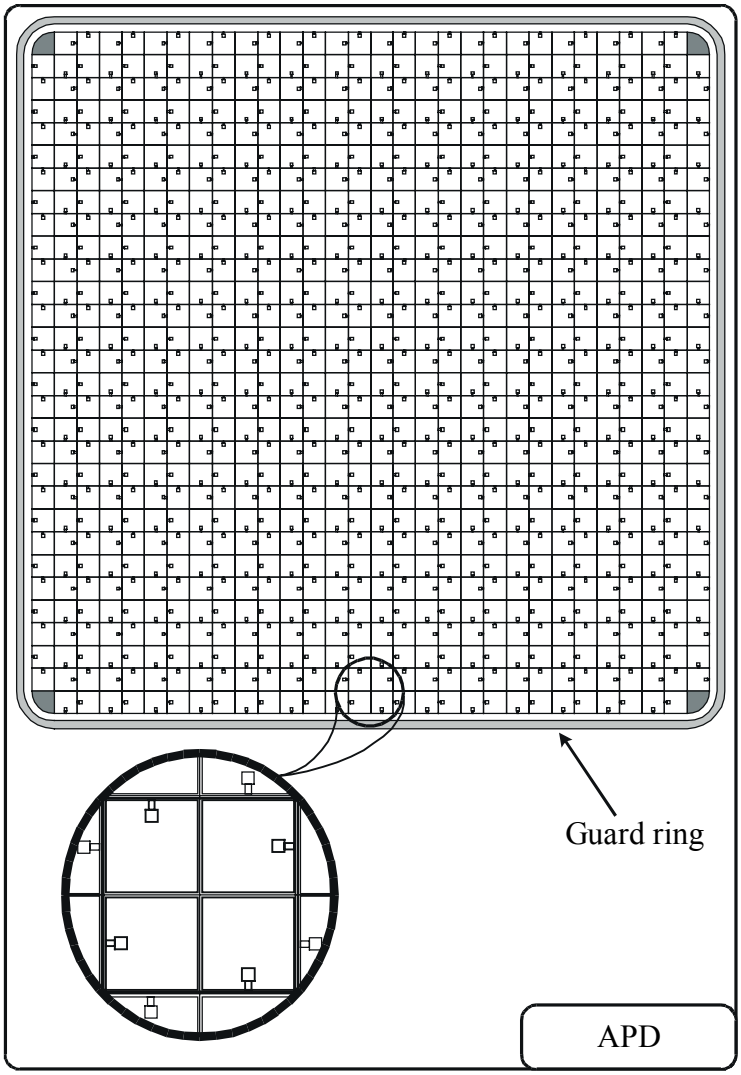
Guard ring
APD

Fig.6

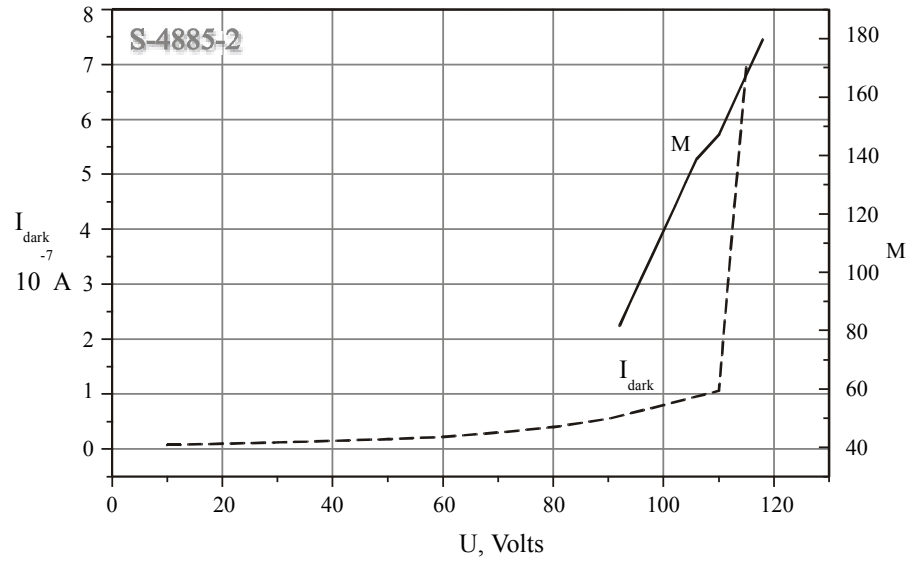
S-4885-2
I dark
-7
10 A
M
I dark
M
U, Volts

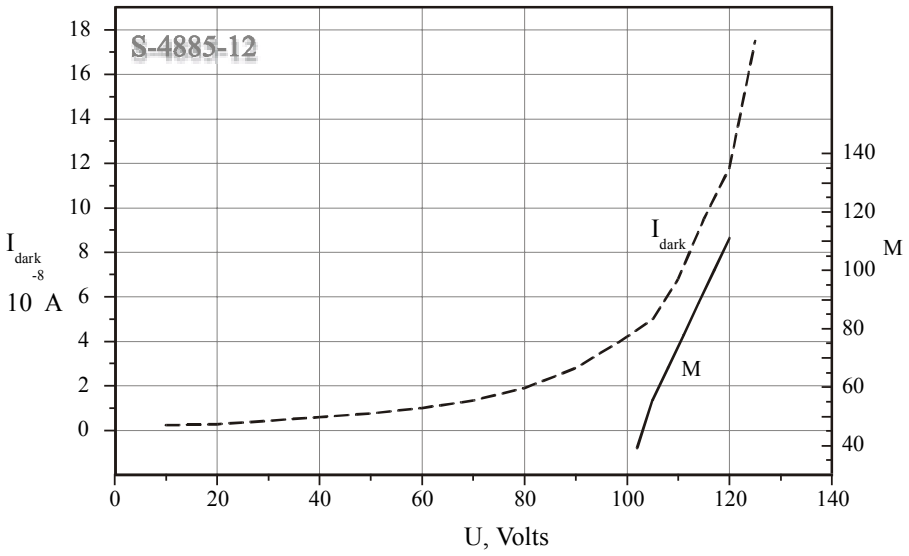
S-4885-12
I dark
-8
10 A
I dark
M
M
U, Volts

Fig.7